Axial Force Negative Stiffness in Axial-Flux Electric Machines

Wen L. Soong[1], Emad Roshandel[2], Zhi Cao[2], Amin Mahmoudi[2] and Solmaz Kahourzade[3]

[1]School of Elect. and Mech. Eng., University of Adelaide, Australia, wen.soong@adelaide.edu.au
[2]College of Science & Engineering, Flinders University, Australia, {emad.roshandel, zhi.cao, amin.mahmoudi}@flinders.edu.au
[3]STEM, University of South Australia, Australia, solmaz.kahourzade@unisa.edu.au

This paper examines the axial force negative stiffness of induction and permanent magnet (PM) axial flux machines. First, simplified analytical models are used to identify the key normalised machine parameters which affect the variation of axial force with airgap length. For current-driven induction machines and PM machines, this is found to be the ratio of the effective magnetic length of the magnets and magnetic core divided by the nominal airgap. For voltage-driven (line-start) induction machines, it is the ratio of the stator leakage inductance to the nominal magnetising reactance. Next, the analytical results are validated against finite-element results and results from experimental axial force testing on induction and PM axial-flux machines.

***Index Terms*—axial-flux machines, axial force, negative stiffness, unbalanced force**

I. Introduction

Axial-flux machines have been of interest in electric transportation applications due to their potential for high torque density and short axial length.

A challenge with the design of these machines is the large axial force between the stator and rotor. In addition, this force increases significantly with decreasing airgap, that is, they can have a large negative axial force stiffness. Surrounding a single rotor with two stators (or vice versa) can minimise the net axial force on the rotor but can result in up to double the negative axial stiffness. This effect becomes more important for larger axial flux machines and may require careful mechanical design and choice of bearings.

The authors recently designed a custom induction motor rotor for a commercial axial-flux PM stator but found when the machine was assembled and energized, that the stator and rotor made contact. This finding provided the motivation for this research into axial force negative stiffness effects.

II. Literature Discussion

When analysing axial forces in axial-flux machines, a number of researchers have used detailed analytical models which can take into account the 3D geometry and often include stator slotting and end-effects [1]–[4]. To include saturation some researchers have used magnetic equivalent circuit models [5], [6] while others have used 3D finite-element analysis [5], [7] for higher accuracy. Most of the work has focused on axial-flux permanent magnet (PM) machines [1]–[8] but there has been some work on axial-flux induction machines (IM) [9], which modeled the effect of static eccentricity on the leakage and magnetizing reactances.

This paper is an extension of an earlier conference paper [10] with added experimental results for force versus gap results for an axial-flux PM and IM.

III. Analytical Force Results

The authors have developed analytical models for the variation of axial force F with airgap l_g for axial-flux machines based on the simplified magnetic circuit models in Fig. 1 [10].

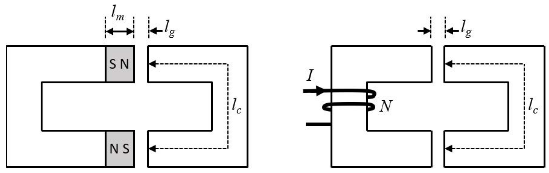

(a) PM-excited (b) Electrically-excited

Fig. 1. Magnetic circuits for the PM- and electrically-excited machine *c*-core configurations [10].

The left model can be used to represent PM machines with a magnet thickness of l_m, and a half magnetic iron path length of l_c. The right model represents induction machines under either current-driven (representing inverter) operation or voltage-driven (representing line-start) operation.

The axial force F as a function of airgap l_g is defined in (1), is proportional to the square of the airgap flux density B_g and is also related to the pole area A and the permeability of free space μ_0.

$$F(l_g) = \frac{1}{2}\frac{[B_g(l_g)]^2}{\mu_0}A \quad (1)$$

For the PM machine and the current-driven IM machine, by analysis of the configuration in Fig. 1 it can be shown that the variation of no-load flux density with airgap is related to the ratio of the parameter l'_{mc} (the sum of the magnetic equivalent length of air corresponding to the PM and stator iron) and the nominal airgap l_{g0},

$$\frac{B_g(l_g)}{B_{g0}} \approx \frac{l'_{mc}/l_{g0}+1}{l'_{mc}/l_{g0}+l_g/l_{g0}} \quad (2)$$

For the voltage-driven IM, from the IM equivalent circuit under no-load conditions it can be shown that the flux density is related to the voltage across the magnetizing inductance and hence to the magnetizing inductance L_m and the stator leakage inductance L_{sl},

$$\frac{B_g(l_g)}{B_{g0}} = \frac{L_m+L_{sl}(l'_c+l_{g0})}{L_m+L_{sl}(l'_c+l_g)} \quad (3)$$

In (3), the magnetic equivalent length of air corresponding to the stator iron l'_c can be estimated from the operating magnetizing inductance L_m and the unsaturated magnetizing inductance L_{m0},

$$l'_c = \frac{(L_{m0}-L_m)}{L_{m0}}l_{g0} \quad (4)$$

IV. EXPERIMENTAL FORCE RESULTS

Experimental axial force tests were carried out using a commercial axial-flux PM machine stator with its PM rotor and also a custom-built IM rotor. For the IM motor testing, the stator is excited with rated DC current. The machines were tested using a precision-controlled civil engineering material testing rig (see Fig. 2). The stator was fixed in position and non-magnetic spacers of known thickness (from 0.22 to 3.8mm) were placed on top of it. The rotor was gradually lowered until it made contact with the spacer and downward pressure was applied to the stator to ensure a uniform airgap. Then upward force was gradually applied to separate the two. The force versus airgap cure was measured and is shown in Fig. 3 for three different spacer thicknesses. The peak force was recorded for each spacer thickness.

Fig. 2. Experimental axial force measurement using a civil engineering material testing rig (left) showing the IM rotor (top right) and PM rotor (bottom right)

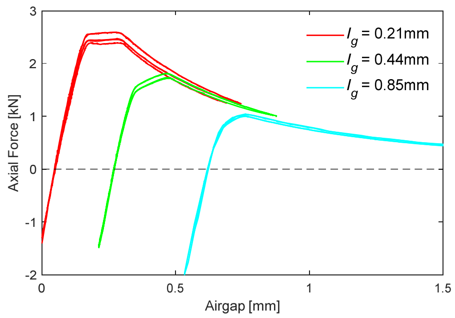

Fig. 3. Measured force vs airgap trajectories for three different spacer thicknesses, the peak force was recorded for each spacer thickness

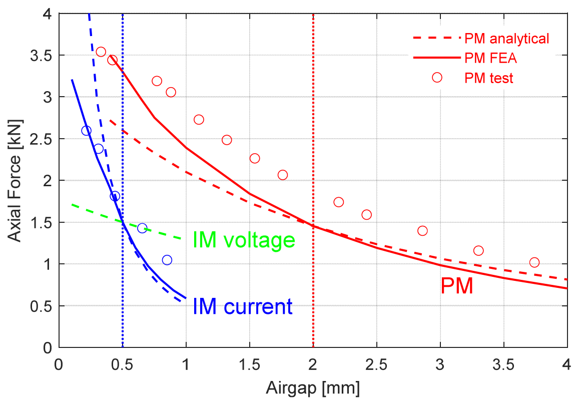

Fig. 4. Axial force versus airgap for the PM (red), current-driven IM (blue) and voltage-driven IM (green) showing the analytical (dashed lines), FEA (solid lines) and test results (symbols). The nominal airgaps are shown by vertical dotted lines. The voltage-driven IM only has analytical results.

Fig. 4 shows the axial force versus airgap results for the three machine types. Test results (circles) are available for the PM machine (red results) and current-driven IM machine (blue results) for a range of spacer thicknesses. These show a similar shape to the 3D FEA results (solid lines) and are generally within about 20%. It is interesting that the measured results are generally higher than the FEA results.

The variation of the force versus airgap of the current-driven IM has a slope (negative stiffness) which is several times larger than that of the PM machine. From (2), this is due to its smaller nominal airgap (0.5mm versus 2mm) and the reduced equivalent magnetic air thickness of the magnets and core l'_{mc}, which is 4mm for the PM machine and about 0.2mm for the IM machine. This may help explain the stator-rotor contact issue in the axial-flux IM prototype mentioned in the introduction.

The analytical results based on (2) and (3) are shown as dashed lines in Fig. 4. As these equations only predict the relative change of force with airgap, the FEA force value at the nominal airgap was used in each case. The analytical results show a reasonable correspondence with the slopes of the FEA and experimental data given the simplicity of the analytical model. The IM current-driven analytical results over-predict the force at small airgaps as only the saturation at the nominal airgap is considered, see (4). The analytical result for the IM voltage-driven case is shown in green. This has a much lower negative stiffness than the current-driven case and is comparable to the PM machine. The lower negative stiffness is related to the voltage excitation, which keeps a more constant airgap flux density despite airgap variations, and is affected by the ratio of stator leakage inductance to magnetizing inductance as shown in (3).

REFERENCES

[1] X. Zhang and B. Zhang, "Analysis of Magnetic Forces in Axial-Flux Permanent-Magnet Motors with Rotor Eccentricity," Math. Probl. Eng., vol. 2021, 2021.

[2] B. Guo, Y. Du, F. Peng, and Y. Huang, "Magnetic Field Calculation in Axial Flux Permanent Magnet Motor With Rotor Eccentricity," IEEE Trans. Magn., vol. 58, no. 9, pp. 5–8, 2022,.

[3] P. Jin et al., "3-D analytical magnetic field analysis of axial flux permanent-magnet machine," IEEE Trans. Magn., vol. 50, no. 11, pp. 11–14, 2014.

[4] Q. Wang, F. Zhao, and K. Yang, "Analysis and Optimization of the Axial Electromagnetic Force for an Axial-Flux Permanent Magnet Vernier Machine," IEEE Trans. Magn., vol. 57, no. 2, pp. 2–6, 2021.

[5] S. M. Mirimani, A. Vahedi, and F. Marignetti, "Effect of inclined static eccentricity fault in single stator-single rotor axial flux permanent magnet machines," IEEE Trans. Magn., vol. 48, no. 1, pp. 143–149, 2012.

[6] A. Parviainen, M. Niemelä, and J. Pyrhönen, "Modeling of axial flux permanent magnet machines," IEEE Trans. Ind. Appl., vol. 40, no. 5, pp. 1333–1340, 2004.

[7] J. Li, R. Qu, and Y. H. Cho, "Effect of unbalanced and inclined air-gap in double-stator inner-rotor axial flux permanent magnet machine," Proc. - 2014 Int. Conf. Electr. Mach. ICEM 2014, pp. 502–508, 2014.

[8] W. Tong, S. Wang, S. Dai, S. Wu, and R. Tang, "A quasi-three-dimensional magnetic equivalent circuit model of a double-sided axial flux permanent magnet machine considering local saturation," IEEE Trans. Energy Convers., vol. 33, no. 4, pp. 2163–2173, 2018.

[9] Z. Nasiri-Gheidari and H. Lesani, "New design solution for static eccentricity in single stator-single rotor axial flux induction motors," IET Electr. Power Appl., vol. 7, no. 6, pp. 523–534, 2013.

[10] W. L. Soong, Z. Cao, E. Roshandel, A. Mahmoudi, and S. Kahourzade, "Unbalanced Axial Forces in Axial-Flux Machines," Australas. Univ. Power Eng. Conf., 2022.